

Multifunctional Structural Energy Storage Composite Supercapacitors

Natasha Shirshova,^a Hui Qian,^a Matthieu Houllé,^b Joachim H.G. Steinke,^a Anthony R.J. Kucernak,^a Quentin P V Fontana,^c Emile S. Greenhalgh,^a Alexander Bismarck,^a Milo S.P. Shaffer^a *

DOI: 10.1039/b000000x

This paper addresses the challenge of producing multifunctional composites that can simultaneously carry mechanical loads whilst storing (and delivering) electrical energy. The embodiment is a structural supercapacitor built around laminated structural carbon fibre (CF) fabrics. Each cell consists of two modified structural CF fabric electrodes, separated by a structural glass fibre fabric or polymer membrane, infused with a multifunctional polymeric electrolyte. Rather than using conventional activated carbon fibres, structural carbon fibres were treated to produce a mechanically robust, high surface area material, using a variety of methods, including direct etching, carbon nanotube sizing, and carbon nanotube in situ growth. One of the most promising approaches is to integrate a porous bicontinuous monolithic carbon aerogel (CAG) throughout the matrix. This nanostructured matrix both provides a dramatic increase in active surface area of the electrodes, and has the potential to address mechanical issues associated with matrix-dominated failures. The effect of the initial reaction mixture composition is assessed for both the CAG modified carbon fibre electrodes and resulting devices. A low temperature CAG modification of carbon fibres was evaluated using poly(3,4-ethylenedioxythiophene) (PEDOT) to enhance the electrochemical performance. For the multifunctional structural electrolyte, simple crosslinked gels have been replaced with bicontinuous structural epoxy / ionic liquid hybrids that offer a much better balance between the conflicting demands of rigidity and molecular motion. The formation of both aerogel precursors and the multifunctional electrolyte are described, including the influence of key components, and the defining characteristics of the products. Working structural supercapacitor composite prototypes have been produced and characterised electrochemically. The effect of introducing the necessary multifunctional resin on mechanical properties has also been assessed. Larger scale demonstrators have been produced including a full size car boot/trunk lid.

Introduction

Despite the progress in the development of electrical energy storage devices, the quest for more efficient, safer systems, with improved specific properties continues, driven by increasing energy requirements. There is a particular need for volume or/and weight savings in mobile products, such as portable electronics or hybrid/electric

vehicles, and aircraft. A particularly promising strategy relies on the development of multifunctional energy storage devices, which offer net savings by combining two conventionally independent sub-systems. One approach simply involves the assembly of two separate components, for example, shaping a battery to fit within a car door. A more challenging but potentially beneficial approach is to develop truly multifunctional devices, built out of multifunctional materials. This paper discusses the possibility of creating a structural material that is also an electrochemical energy storage device. The structural performance, here, is not just about robustness, but involves carrying significant mechanical loads in service. This concept was motivated by the observation that carbon-based materials are both the leading structural reinforcement and a common electrode component, and that both structural composites and electrochemical devices are typically laminates. The question is the extent to which these functions can be unified.

Many different electrical energy storage mechanisms could be considered. However, here the focus is on the development of multifunctional supercapacitors, since they offer useful performance, for example in load-levelling of high power applications, without involving significant changes of electrode shape or volume. Electrochemical double layer capacitors consist of two high surface area electrodes separated by a thin electrically-insulating but ionically-conducting electrolyte. To create a structural supercapacitor, at least two multifunctional components are required, a structural reinforcement/electrode, and a structural separator/electrolyte. Both aspects are discussed in more detail below.

Supercapacitor electrodes must have high, ionically-accessible surface area, good conductivity, as well as thermal and (electro)chemical stability. There are a number of publications¹⁻⁴ which discuss possible materials and methods of their synthesis and modification, however, carbon in a variety of activated forms remains the most common choice. Structural carbon fibres are widely used in composite systems that exploit their high strength and stiffness⁵ and good electrical conductivity². However, structural carbon fibres have very low surface area, whilst industrial activated carbon fibres are usually poorly graphitised and lack the required properties. Instead, a means of increasing the effective surface area of structural carbon fibres is required. A number of possible modification methods can be considered, including physical and chemical activation, introduction of carbon nanotubes and impregnation with carbon aerogel, as discussed and compared further below.

The multifunctional electrolyte may be even more challenging, since it must combine high ionic conductivity with excellent rigidity and strength. Unfortunately, it is generally accepted that ionic conductivity and mechanical performance have an inverse relationship, since ionic conductivity requires molecular motion and rigidity does not.⁶⁻¹⁰ Nevertheless, it is possible to obtain electrolytes with an unexpectedly good balance of performance by designing a bicontinuous structure⁶ where one phase is responsible for the mechanical properties and a second phase provides ionic conduction. A more conventional, simple molecular interpenetrating network (molecular mixture) does not adequately isolate the two property requirements, and the phase separation should occur on a longer lengthscale, most likely defined by the other components in the device. The most effective existing examples use epoxy as the structural component and ionic liquid based electrolyte as a second phase.^{6, 7, 11, 12} Both of these choices excel at their attributed role. Epoxies have high mechanical performance in combination with chemical and thermal stability^{13, 14} whereas ionic liquids have good ionic conductivity, a wide electrochemical window, negligible

vapour pressure and high thermal stability¹⁵⁻¹⁷. Moreover, there is great variety in types of both materials; for example, epoxy resins may contain two or more oxirane groups and a wide range of hardeners are available, and ionic liquids can combine a wide variety of cations and anions. Systems can therefore be tuned to produce the desired phase behaviour, required to manifest the complementary properties, although formulation can be difficult as illustrated below.

This paper illustrates the development of a structural supercapacitor system based on laminates of activated structural carbon fibre fabric electrodes sandwiching a structural glass fibre separator filled with (structural) electrolyte. The results show a comparison of different activation methods, and various approaches to developing an optimised, processable system. The data highlight the importance of bicontinuous microstructures for both electrodes and electrolytes. A range of proof of concept demonstrators have been fabricated, and the prospects for further progress are discussed.

15 Experimental Part

Materials

Plain weave carbon fibre fabric (HTA, Toho Tenax) was used for the modification and as electrodes for structural supercapacitors (Tissa Glasweberei AG 862.0200.01) with an areal density 200 g m^{-2} and thickness of 0.21 mm and a glass fibre fabric (plain weave, 200 g m^{-2} , 842.0200.01, TISSA Glasweberei AG) was used as separator. The resorcinol-formaldehyde resin AX2000 was kindly provided by INDSPEC Chemical Corporation.

Poly(ethylene glycol)diglycidyl ether (PEGDGE, $M_n=526$, Aldrich), triethylenetetraamine (TETA, technical grade, Aldrich) 1-ethyl-3-methylimidazolium bis(trifluoromethylsulfonyl)imide (EMITFSI, purity $\geq 98\%$), bis(trifluoromethane)sulfonimide lithium salt, LiTFSI, (puriss., $\geq 99.0\%$ (19F-NMR) Aldrich), KCl (Sigma-Aldrich), EDOT (Sigma-Aldrich), NaPSS (Mw 70kDa, Sigma), $\text{Fe}(\text{NO}_3)_3 \cdot 9\text{H}_2\text{O}$ (Sigma), FeCl_3 (Sigma), cobalt acetate ($\text{Co}(\text{CH}_3\text{COO})_2 \cdot 4\text{H}_2\text{O}$, Sigma-Aldrich), ethanol (puriss. $>96\%$, Sigma-Aldrich). Three fully formulated, commercially available, high performance, epoxy resins with trademarks MVR444 and toughened MTM57 and VTM266 were prepared at Cytec Industrial Materials. All chemicals, including solvents for extraction were used as received.

Modification of carbon fibres

The modification of carbon fibres were described in detail elsewhere, for example chemical/physical activation of carbon fibres^{18, 19}, grafting CNT onto carbon fibres²⁰, as well as preparation of structural electrolytes based on commercial epoxy resins.^{6, 10} CAG modification of the carbon fibres was performed as follows; Resorcinol-formaldehyde (RF) polymer was prepared using a commercially available RF resin (AX2000, INDSPEC Chemical Corporation). The AX-2000 resin contains about 73.1 wt % resorcinol at a R:F molar ratio of 2:1. Potassium hydroxide (KOH) was used as the catalyst (C) and the R:C molar ratio was 50:1. Additional formaldehyde (37 wt % solution) was added to the mixture to keep the R:F ratio at 1:2. The weight percentage of the RF in the mixture was controlled to be 25%, 40% or 50% by adjusting the quantity of the diluent distilled water. The mixture was tightly sealed and stirred for 2 h. RF solution was infused into the carbon fibres using Resin Infusion under Flexible Tooling (RIFT) method at room temperature. Specimens were then cured for 24 h, dried, placed into a chamber furnace (Lenton ECF 12/30) with a gas tight Inconel

metal retort (Lenton 'A105') and carbonised in the inert atmosphere (constant N₂ flow at 0.5 l/min) at 800°C for 30 min.

As carbon fabrics are capable of withstanding high temperatures, especially under non-oxidizing atmospheres, it is possible to perform a direct growth of carbon nanotubes by Catalytic Chemical Vapor Deposition (CCVD). This growth is achieved by using a previously deposited catalytic phase on the surface of the carbon fabrics. Previous work^{20, 21} has already shown that such process are able to provide homogeneous coverage of the carbon fabric by a layer of CNTs, giving rise to a hybrid composite with high specific surface area. Grafting of CNTs on CFs was performed as follows. Fabrics were heated at 80°C in a ventilated oven (Binder) for 2 h before any treatment to remove any adsorbed moisture that would prevent proper grafting of the CNTs over the carbon surface. A precursor solution of metallic salts was prepared using iron nitrate (Fe(NO₃)₃·9H₂O), and cobalt acetate (Co(CH₃COO)₂·4H₂O) dissolved in a mixture of distilled water and ethanol. Carbon fabrics were impregnated with the catalyst precursors solution and then left to dry in open air at room temperature overnight. After complete drying, pieces of fabrics were placed in a tubular oven (Carbolite) and heated up in inert atmosphere (N₂) to the reaction temperature used for the growth process (750°C). Once heated to the suitable temperature, a mixture of gaseous reactants was introduced in the reaction chamber to initiate the CNT-growth process. Nitrogen, ethylene and hydrogen were used in volume proportions of 50:40:10 for a total gas flow of 4 L/min. Accurate feeding of the gas flows was realised with mass flow controllers (Bronkhorst). Ethylene acts as carbon source while hydrogen prevents excessive self-cracking of ethylene and promotes catalyst lifetime. Nitrogen is added to the gas stream to dilute reactive gases and ensure a homogeneous growth of CNTs on all the carbon fibres. Finally, the reaction was continued for a defined time (5 to 20 min) until the desired yield of growth was achieved (from 5wt% up to more than 20 wt%). Once CCVD synthesis was completed, the fabrics were left to cool to room temperature under inert atmosphere.

Sizing of carbon fabrics with CNTs was also performed as follows. Fabrics were impregnated with a specifically designed formulation (Aquacyl™ custom, Nanocyl) containing 3 wt.% of NC7000™ carbon nanotubes (Nanocyl) as well as a polymeric dispersing agent. The thickness of impregnation was controlled using a bar coater of 200 μm (BYK) to ensure homogeneous deposition of the sizing solution over the fabric surface and the excess of solution was removed. The so-coated fabric was dried at room temperature for 2 h and then placed in a ventilated oven (Binder) at 120°C for 2 additional hours to guarantee complete evaporation of water. After drying, the fabrics were removed and cooled down to RT before a second impregnation step. The second stage of impregnation was performed using the same protocol, again using a wet-coating thickness of 200 μm. The wet sample was then dried at RT for 2 h and at 120°C for 2 extra hours. Fabrics were transferred to another oven (Bouvier-Technofour) that was heated up to 450°C at a rate of 2°C/min under a steady flow of air (1 L/min). Heating to 450°C triggers the complete decomposition of the dispersing agent while the carbon nanotubes remain unharmed by the heat treatment. This thermal decomposition engenders the formation of a carbonaceous deposit that helps to anchor the CNTs onto the CF surface. Sized fabrics were recovered after complete cooling.

Further modification of the CAG-modified carbon fibres

The CAG modified carbon fibres were further modified by PEDOT using two formulations.^{22, 23} For the first (PEDOT 1), 0.3 g NaPSS (Mw 70 kDa, Sigma) were dissolved in 15 ml H₂O followed by addition of 0.21 g EDOT (Sigma). Components were homogenised using ultrasonic probe for 15 s to form a milky emulsion and 14.8 g Fe(NO₃)₃·9H₂O in 10 ml H₂O added to the solution. The mixture was vigorously stirred using a magnetic stirrer for 5 s. The carbon fibres were submerged into the formed mixture for 5-10 min and then placed onto a PTFE coated film for 24h. Afterwards the carbon fibres were placed into 0.1M HCl for 1 week followed by washing with water and ethanol and drying until constant weight.

For the second route (PEDOT 2), equal amounts of EDOT and FeCl₃ (0.25 g) were dissolved in 5 ml EtOH and mixed. Carbon fibres were submerged in this solution for 5 min and then left at room temperature (21°C) for reaction to proceed. After 1 h carbon fibres were washed in EtOH to remove unreacted reagents and dried until constant weight.

Characterisation of modified carbon fibre fabrics

Morphology and Surface Characterization of CAG Modified Carbon Fibre Fabrics.

The microstructure of the carbon fibre fabrics was characterized using a field emission gun scanning electron microscopy (SEM) (Gemini LEO 1525 FEG-SEM, Carl Zeiss NTS GmbH), operating at 5 kV, without metal coating. Specific surface area and pore size of the modified carbon fibres were studied using a Micromeritics TriStar 3000 analyzer (Micromeritics UK Ltd.) by pure N₂ adsorption. The data were analysed using the Brunauer, Emmet, Teller (BET) and the Barrett, Joyner and Halenda (BJH) methods.

Electrochemical Characterization of Modified Carbon Fibre Fabrics

Electrochemical tests were performed on the carbon fibre fabric tows (~3k extracted fibre bundles, around 3.5 cm long) before and after the modification at ambient temperature, using a three-electrode cell (platinum wire counter electrode, silver-silver chloride (Ag/AgCl) reference electrode) filled with 3 M KCl aqueous electrolyte. Cyclic voltammetry (CV) experiments were conducted between -0.2 and +0.2 V, using a potentiostat SI 1287 (Solartron Instruments). The scan range was chosen for this work as it provided representative capacitance results and allowed for quick comparison between different modified carbon fibres. The specific capacitance was calculated from the current $(I_a - I_c)/2$ at 0 V, i.e. average of the current from the anodic and cathodic part of the curves.

Fabrication of structural supercapacitors

To manufacture structural supercapacitors, different matrix/electrolyte mixtures of PEGDGE:TETA (90 wt.%, molar ratio 3:1) and ionic liquid, EMITFSI (10 wt.%) were used. Mixtures were degassed before infusion using resin infusion using flexible tooling (RIFT) under 1 bar. The layout for producing structural supercapacitors consisted of two carbon fabric electrodes, which sandwiched two glass fabrics as the separator (mirrored at the midplane to ensure the laminates were symmetrical, for mechanical testing).¹⁸ Copper tape (with conductive adhesive, 542-5511, RS components) was applied to the carbon fibre fabrics to form the current collector for electrochemical characterization. The laminates were cured at 80°C for 24 h.

Characterisation of structural supercapacitors

Mechanical properties

The in-plane shear properties of the structural supercapacitors were investigated by tensile testing²⁴ of a $\pm 45^\circ$ laminate according to ASTM standard D3518. The composite specimens were dry cut to dimensions of 150×25 mm. Glass-fibre composite end-tabs were then applied to both ends of each specimen, resulting in a gauge length of 90 mm. A biaxial strain gauge (FCA-5-11, Techni Measure) was adhered to the sample using cyanoacrylate glue at the midspan of the specimens to measure the strains in both the longitudinal and transverse directions. The tests were conducted at room temperature using an INSTRON 4505 universal testing machine, equipped with a 1 kN load cell, at a crosshead speed of 2 mm min^{-1} . A minimum of five measurements were conducted for each type of specimen. The fibre volume fraction of the reinforcements in the composites was measured²⁵ according to Method II of the standard ASTM D3171.

Electrochemical properties

Charge-discharge experiments were performed at room temperature using a 0.1 V step voltage applied for 10 s and calculations performed as described elsewhere.¹⁸

Characterisation of structural electrolyte

To study the morphology of the structural electrolyte, EMIM-TFSI and LiTFSI were extracted from the cured formulations as follows. Pre-weighed structural electrolyte, about 0.5 - 1.0 g, was placed in a glass vial filled with ethanol which was changed twice a day for at least one week, and subsequently dried in an oven at 70°C under reduced pressure, to constant weight.

SEM images of extracted samples were recorded on a Jeol JSM 5610 LV scanning electron microscope with an accelerating voltage of 15 kV, after gold sputter coating for 120 s in an argon atmosphere.

Ionic conductivity was determined using impedance spectroscopy (Solartron 1260) in the frequency range 10^5 -0.1 Hz.

3 Results and Discussion

3.1 Comparison of methods for carbon fibre modification

Woven carbon fibres mats were modified using number of different treatments and compared to identify the most promising performance (**Fig. 1**); the goal is to provide a maximum increase in electrochemical surface area whilst retaining the mechanical properties of the pristine carbon fibres. The examples shown have relatively little deterioration of mechanical performance^{19, 20, 26}, unlike many types of activation^{19, 27-30} or nanotube grafting²¹. Carbon fibres annealed in inert atmosphere are included as a control since many methods include heat treatment, either for growing nanotubes or removing sizing or surfactant. The most straightforward approach is simply to activate the surface of the structural fibres using an etching process. After a study of various activation chemistries, chemical activation of carbon fibres using KOH was found to produce the best results¹⁹ (**Fig. 1**). In this case, the surface of carbon fibres appeared etched (**Fig. 2**) creating mesopores¹⁹ responsible for the increase of the surface area and specific capacitance (**Fig. 1**). However, the increase is limited to a relatively small volume, since the fibre core must remain broadly intact for reinforcement purposes. The addition of nanostructures to the carbon fibre surface, therefore, offers better prospects for increasing the capacitance.

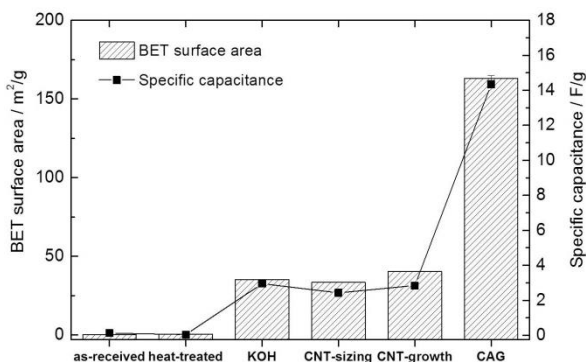


Fig. 1 Effect of different types of carbon fibres modifications on BET surface area and specific capacitance of CF/GF/CF composite. (Electrolyte used – 3M KCl; specific capacitance was calculated from cyclic voltammetry, range -0.2V - +0.2V, scan rate 5 MV/s)

5

The introduction of carbon nanotubes (CNTs) onto carbon fibres is known to increase their surface area²⁰; intrinsically the use of CNTs is appealing as, in principle, they offer high surface areas and excellent mechanical performance. There are examples of pure CNT fibres with promising performance, but currently only very small amounts of material are available³¹⁻³³. The combination of CNTs with carbon fibres to form hierarchical composites is very promising for a variety of structural and functional purposes²¹, and is already commercialised in some cases. As well as providing the necessary electrode performance, the addition of transverse CNTs onto unidirectional fibres may inhibit matrix-dominated failure processes prevalent in carbon fibre composites; tackling matrix dominated failures is likely to be particularly important in the structural electrical energy storage context, since multifunctional electrolytes/matrices are likely to be mechanically less robust than conventional resins. CNTs can be dispersed at low concentrations in the matrix, or attached to the primary carbon fibres by growth or post-growth coating processes. Since connection to the primary carbon fibre electrodes is key, these latter options are most relevant; two possible examples have been tested here. In the first case, the carbon fibres were impregnated with a CNT sizing, followed by pyrolysis of surfactant/binder. In the second, the CNTs were grown directly from the surface of carbon fibres, using CCVD. The impregnation process is simpler to implement, and relates to a large number of possible variants, such as electrophoretic deposition or chemical grafting. The disadvantage from a mechanical point of view is that the CNTs typically lie predominantly parallel to the carbon fibre surface and likely offer less transverse contribution to matrix properties. The initial improvement using the CNT sizing was very minor (**Fig. 1**); however, to remove the binder/surfactant, to allow electrolyte access to the hybrid electrode, and to ensure good electrical connection, the CNT impregnated carbon fibres were subjected to pyrolysis. SEM (**Fig. 2d**) shows a homogeneous coverage of the carbon fibres with a layer of CNTs, consistent with the observed increase in surface area and capacitance (**Fig. 1**). CVD growth of CNTs from the surface of carbon fibres, initiated by the use of pre-deposited metal catalyst, avoids the presence of a (pyrolyzed) binder and may improve CNT anchoring. Again a uniform covering of carbon fibres forms but with a more three dimensional microstructure than for the pyrolysed system, leading to a further improvement in accessible surface area. Etching of the carbon fibre by the metal catalyst during growth

tends to degrade primary mechanical properties but the effects can be limited by careful choice of parameters²¹.

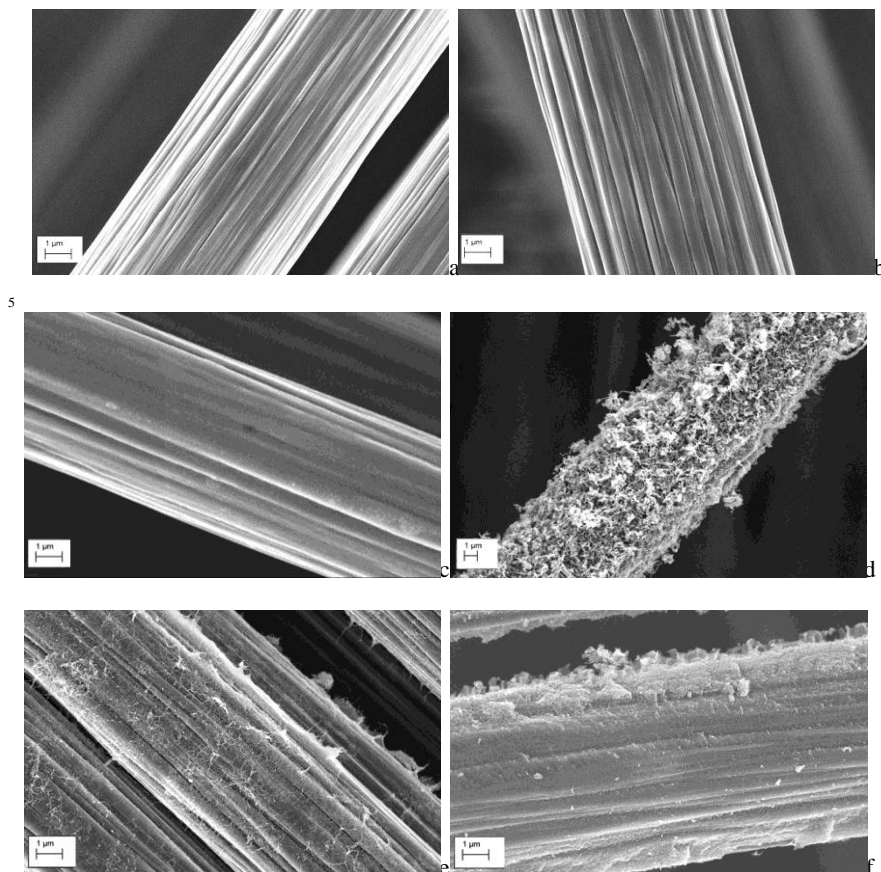


Fig. 2 Scanning electron micrographs of (a) as-received, (b) heat-treated, (c) KOH activated carbon fibres, (d) CNT grafted carbon fibres, (e) CNT sized carbon fibres, (f) CAG modified carbon fibres.

Whilst CNTs are intrinsically promising, the embodiments discussed have either limited volume, or relatively low CNT packing density, or both. The net contribution of the CNT layer is, therefore, low. A simple geometric model indicates that a significant increase in accessible area is possible, in principle, using small diameter nanotubes at high packing densities (**Fig. 3**). The nanotubes cannot be too small, or they will tend to bundle and leave insufficient space to accommodate the electrochemical double layer; they cannot be too long as they will limit the fibre packing efficiency. An optimum will exist for nanotubes with diameters of ~3-5nm, lengths <10 μm, and a relatively high packing density. Fig. 3 is plotted for an areal packing density of around 15%; higher packing density might be possible, but space is needed for the electrolyte and electrochemical double layer. Unfortunately, despite progress in preparing dense small diameter CNT arrays for vias in microelectronics³⁴, conditions to prepare such a structure grafted on carbon fibres remain elusive.

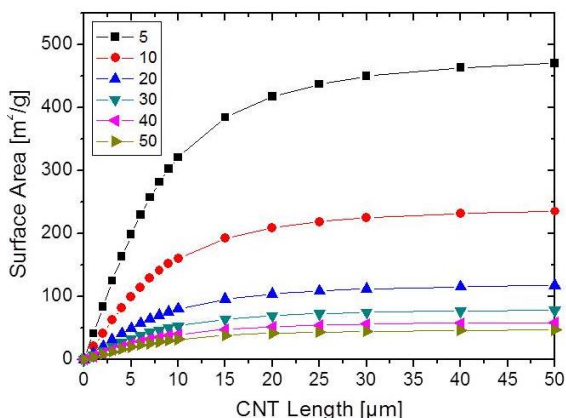


Fig. 3 Simple geometric estimate of potential surface area of the CNT modified carbon fibres depending on the CNT length, as a function of different diameters (given in nm). These data are for a 15% surface coverage.

As an alternative, a three-dimensional carbon aerogel (CAG) can be formed around the carbon fibres²⁶, filling all the available free volume with a bicontinuous, electrically-connected structure with high surface area and low density. CAG is formed *via* a sol-gel process between organic precursors, for example resorcinol (RF) and formaldehyde (FA), in the presence of the catalyst, resulting in the highly crosslinked organic gel, which after pyrolysis a forms highly porous carbon network.^{35, 36} CAG is often used as a pure supercapacitor electrode material. In addition, the combination with non-structural, low density, short carbon fibre felts has been shown to minimise shrinkage, simplify handling, and maximise electrochemical performance.^{37, 38} The unexpected combination with high loadings of continuous structural fibres, retains these advantages, and introduces additional mechanical benefits through the formation of a monolithic supportive matrix network.

Of the methods studied, the CAG-modified carbon fibres showed greatest potential for improving surface area and electrochemical double layer capacitance, whilst retaining the structural performance of the primary fibres. The method increased the surface area and specific capacitance by three orders of magnitude over the initial structural fibres, as well as fivefold and fourfold, respectively, over the next best approach, using KOH activated carbon fibres (**Fig. 1**). In principle, the physical and mechanical characteristics of the CAG are determined by the geometry and length scales of the structures, which can be modified³⁹⁻⁴¹ by varying synthesis parameters, including concentration of catalyst, concentration of resorcinol, ratio of resorcinol to formaldehyde and temperature.

3.2 Effect of resorcinol/formaldehyde concentration on the properties of the modified carbon fibres

In the context of structural supercapacitors, the volume fraction of primary reinforcing fibres should be kept high (>40 vol% of the woven carbon laminates), and thus the volume available for loading with CAG is limited. Since the volumetric capacitance of CAG is nearly related to CAG density and the amount of active material¹, it was decided to vary concentration of the RF in the reaction mixture⁴² keeping all other parameters constant, including R:F, precursor to catalyst ratio as well as temperature

and time. A set of CAF-CF laminates were prepared, infused with varying RF concentration, and the performance assessed. A steady increase of the BET surface area was observed as concentration of RF was increased from 20 wt% to 50 wt%, as a result of the increase in the volume of both mesopores (from 20 to 40 wt%) which can be seen as an increase in hysteresis between the adsorption and desorption isotherms (Fig. 4) and micropores (from 40 to 50 wt%). The literature data describing the dependence of BET surface area upon RF concentration is not consistent, ranging from not affected⁴³, to decreased^{35,42} and increased^{44,45}. These variations can be attributed to other experimental parameters such as the type and amount of catalyst, or the carbonisation conditions (temperature and time). However, a detailed comparison of the literature data is outside of the scope of this paper.

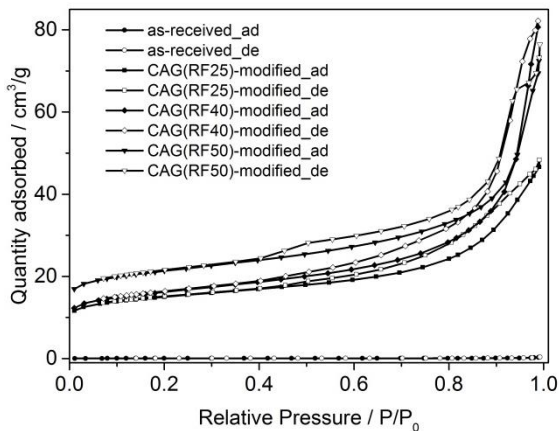


Fig. 4 Adsorption/desorption isotherms of as-received carbon fibres and carbon fibres infused using different concentrations of RF.

15

As expected, the CAG loading in the carbon fibre fabrics increased with increasing infused RF concentration. The decrease of the RF concentration from 40 wt% to 25 wt.% led to a decrease of the CAG loading in the resulting modified carbon fibres and associated reduction of the specific capacitance (Table 1)⁴¹. The slightly greater than proportionate loss of CAG loading may be due to dilution of the reaction mixture leading to a reduction of the polycondensation rate⁴³ and yield of the reaction. The decrease in the volume of mesopores, associated with the decrease of the RF concentration, may also contribute to the loss of capacitance^{43, 44}. The increase of the RF concentration to 50 wt% led to an increase of the CAG loading and an increase of the surface area, due to a reduction of pore size (Fig. 5) but it did not increase specific capacitance. Clearly, many of the smaller pores formed at higher RF concentrations are too small to allow effective electrolyte access, and the more open 40wt% structure is more favourable. The more open structure likely offers further advantages in improved ion transport.

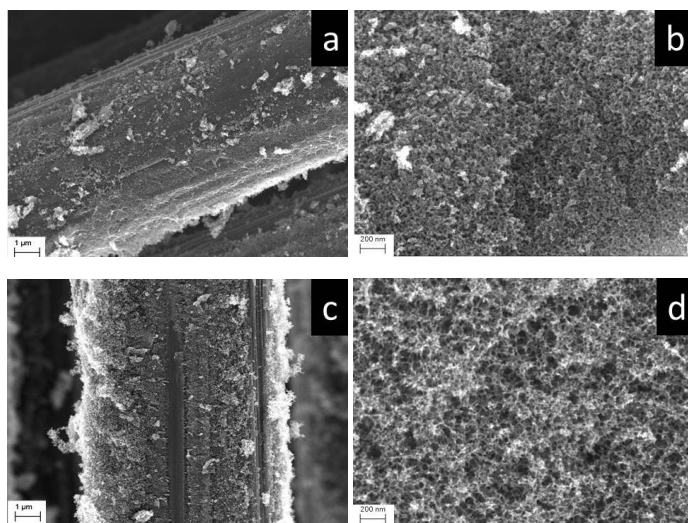
30

Table 1 Effect of the RF content in the sol on properties of resulting CAG modified carbon fibres

| RF concentration, wt% | CAG loading, wt% | BET surface area, m ² /g | Pore width, nm | Specific capacitance, ^a F/g |
|-----------------------|------------------|-------------------------------------|----------------|--|
| 25 | 6.0 | 51.7 ± 0.5 | 5.2 | 3.8 ± 0.1 |
| 40 (initial conc) | 9.1 | 56.1 ± 0.5 | 7.3 | 7.4 ± 0.3 |
| 50 | 12.9 | 73.2 ± 0.8 | 5.5 | 4.0 ± 0.2 |

^a Electrolyte - 3M KCl; specific capacitance was calculated from CV measurements using the three electrode setup in the voltage range -0.2 to 0.2 V at scan rate 5 mV/s.

5 The change in pore size observed is consistent with previous investigations into the formation mechanism of these CAG microstructures^{40, 46}. There are two possibilities for phase separation, i.e. the formation of a porous structure, during resorcinol-formaldehyde polycondensation, depending on RF/W ratio and concentration of catalyst in the sol. One of them is nucleation-growth, which upon increase of
 10 resorcinol concentration may become a spinodal decomposition^{40, 46}. It is reasonable to assume that for the system studied, the transition occurs between RF concentration 40 wt% and 50 wt% leading to observed changes in the morphology. Similar findings were reported by Schwan and Ratke⁴⁰ on an example of resorcinol-formaldehyde polycondensation catalysed using sodium carbonate and nitric acid. They observed
 15 that even small variations in the water content led to significant differences in the mechanical performance of the CAG formed which was attributed to the change in the phase separation mechanism. However, no mechanism transition was reported by Szczurek et al.⁴⁴ and a steady decrease of the surface area as well as porosity was reported for CAG produced from cured resorcinol-formaldehyde resins synthesised
 20 with higher RF concentrations. It was also reported³⁵ that increases in RF/W lead to increased pore polydispersity which has a negative effect on the double layer capacitance.⁴⁷



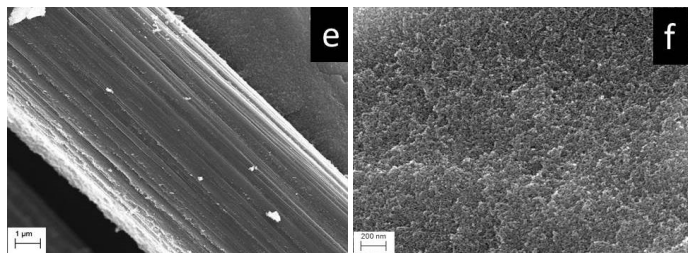


Fig. 5 Scanning electron micrographs of CAG modified carbon fibres prepared using different amounts of RF (a, b) 25 wt%, (c, d) 40 wt% (d, e) 50 wt%. For each sample, two different magnifications are presented.

Fig. 6 shows typical cyclic voltammograms (CVs) of CAG modified carbon fibres in 3M KCl solution over a potential range of -0.2V to $+0.2\text{V}$. All curves exhibit a nearly rectangular shape consistent with expected capacitive behaviour. The specific capacitance from cyclic voltammetry was calculated from the current $(I_a - I_c)/2$ at 0V , i.e. average of the current from the anodic and cathodic part of the curves. CAG modified carbon fibres prepared from the mixture containing 40 wt% RF displayed the highest current density as a result of the presence of larger pores.

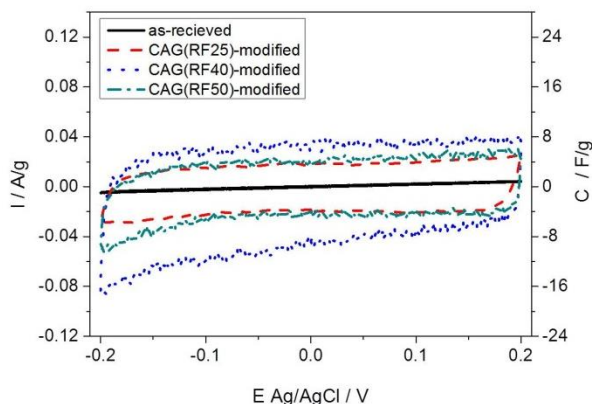


Fig. 6 Cyclic voltammetry response for CAG/GF/CAG composites in 3M KCl depending on the amount of the resin in the sol formulation. Scan rate – 5 mV/s

15

3.3 Multifunctional performance of the composites based on CAG-modified carbon fibres

Composite electrodes manufactured using CAG-modified carbon fibres were considered to have properties required for structural supercapacitors, i.e. high strength and electrochemical surface area. Structural supercapacitor laminates containing 40 wt% CAG-modified carbon fibres have been demonstrated, using woven glass fibre separators and a multifunctional electrolyte matrix.²⁶ Using the same multifunctional polymer electrolyte, which comprised of polyethylene glycol diglycidyl ether (PEGDGE) and 1-ethyl-3-methyl imidazolium bis(trifluoromethylsulfonyl)imide (EMIM-TFSI), structural supercapacitor composites were manufactured using CAG-modified carbon fibres with different RF content in the sol initially infused.

The specific capacitance of the composites was calculated from charge-discharge

experiments with a step voltage of 0.1 V and charging time of 60 s and the values overall (**Table 2**) follow the trend observed for the liquid electrolyte measurements (**Table 1**). However, there is a very significant decrease in the apparent specific capacitance which may be attributed to changes in wettability, segregation of the multifunctional electrolyte components at the electrode interface, or the availability of ions. Furthermore, the ionic conductivity of the polymer electrolyte is much lower than that of the liquid aqueous electrolyte; the ionic conductivity of PEGDGE epoxy containing 10 wt% ionic liquid electrolyte is $2.8 \cdot 10^{-2}$ mS/cm, compared to above 90 mS/cm for 3M KCl. As discussed further below, improvements in the multifunctional electrolyte are required.

Mechanically, the primary structural fibres, which are thought to be relatively unaffected by the CAG modification, determine the in-plane tensile performance of these structural devices; the tensile performance is, therefore, expected to be excellent, since the composite performance is “fibre-dominated”. A more interesting, less obvious question is whether the matrix-dominated properties will be improved or degraded. Given the limited amount of material available, it was decided to focus on matrix-dominated composite tests, as a more demanding and informative evaluation of the different systems; specifically, an in-plane shear test was chosen to evaluate the effect of CAG-modified carbon fibres properties on the fibre/matrix interface. In this study, CAG can be potentially considered to be a matrix reinforcement²⁶. Indeed, the introduction of CAG significantly improves in-plane shear modulus, which rises monotonically with CAG (reinforcement) content (**Table 2**). However, the relative increase is smaller at the higher CAG loadings, suggesting that the coarse 40 wt% RF-derived CAG structure, with thicker struts, is relatively more effective at stiffening. The in-plane shear strength of the manufactured structural supercapacitors was less affected by presence and amount of CAG, although it begins to decrease at the highest CAG loading.

Table 2 Effect of the resin content in the sol formulation on the electrochemical properties and in-plane shear response by testing of the structural supercapacitor devices based on CAG-modified carbon fibres

| RF concentration, wt. % | CAG loading (%) | C_g (mF/g) | ESR ($k\Omega \cdot cm^2$) | Shear Strength τ_{12}^{m} (MPa) | Shear Modulus G_{12}^{chord} (MPa) | Vol Reinforcement (%) |
|-------------------------|-----------------|--------------|------------------------------|--------------------------------------|--------------------------------------|-----------------------|
| 0 | - | 12.5 | 120.8 | 5.36 ± 0.07 | 276 ± 14 | 47.2 |
| 25 | 6.0 | 73.1 | 82.1 | 6.02 ± 0.25 | 686 ± 68 | 42.0 |
| 40 | 9.1 | 90.5 | 79.2 | 9.78 ± 0.08 | 1172 ± 112 | 42.0 |
| 50 | 12.9 | 88.0 | 80.2 | 7.94 ± 0.60 | 1379 ± 116 | 42.0 |

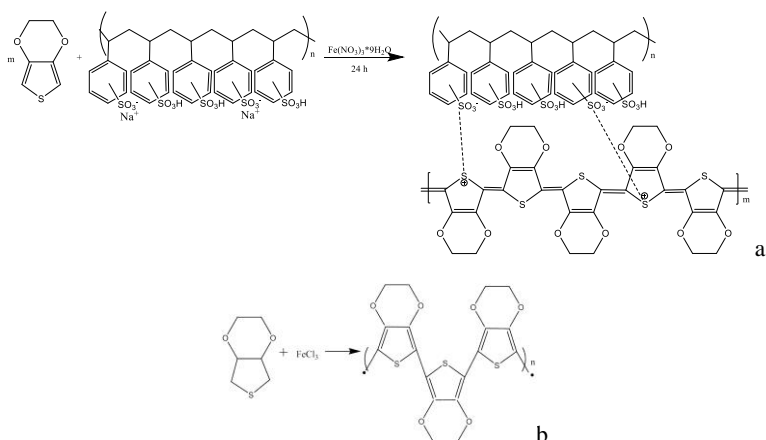
^a Electrolyte - PEGDGE with 10 wt% IL; separator – GF.

3.4 Further improvement of CAG modified carbon fibres

The data presented above confirm that the CAG-modified carbon fibres prepared from the sol containing 40 wt% RF showed the most promising results, so far. Whilst further optimisation is clearly possible, there does appear to be a balance between CAG-content, mechanical performance and electrochemical accessibility. Within the available volume, there will be an optimum microstructure for pure electrochemical double layer capacitance somewhere near the current system. To improve performance

even further, additional modification of the CAG-modified carbon fibres could be performed using one of the available methods, including physical (oxidation) or chemical (KOH) activation, or the introduction of pseudo-capacitive components, such as metal oxides⁴. However, all these methods require high temperature treatment, making the introduction of a pseudo-capacitive component based on conducting polymer an attractive alternative.^{3, 4, 23, 48} Among the most commonly studied conducting polymers, in this context, are polypyrrole (PPy),^{48,49} polyaniline (PANI),⁵⁰ poly(3-methylthiophene) (PMET)⁵¹ and poly(3,4-ethylenedioxythiophene) (PEDOT)^{52, 53}. In this research, PEDOT was chosen²³ because of its high conductivity, good electrochemical and mechanical properties as well as environmental and thermal stability.

There are a number of methods reported in the literature for polymerisation of EDOT^{22, 52, 54}, including electrochemical polymerisation⁵²; room temperature emulsion (co)polymerisation of EDOT with NaPSS in the presence of $\text{Fe}(\text{NO}_3)_3$ (Scheme 1a)²² and room temperature polymerisation in FeCl_3 -methanol solution (Scheme 1b)²³. For preliminary studies, the two last methods have been explored, as shown in **Scheme 1**.



20

Scheme 1 Reactions used to synthesise PEDOT

Both methods still require optimisation but preliminary studies showed that a two fold improvement in the specific capacitance can be achieved when CAG-modified carbon fibres are subjected to EDOT polymerisation (**Fig. 7**). However, further optimisation is required in order to maximise contribution of PEDOT.

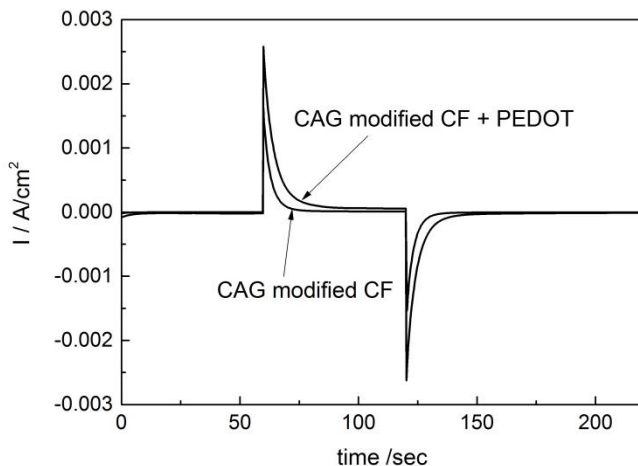


Fig. 7 Charge-discharge curves of the CAG modified carbon fibres before and after modification with PEDOT2. Step voltage 0.1 V. Electrolyte 3M KCl.

5 3.5 Multifunctional electrolyte

The discussion so far has concentrated on the development of structural electrodes via modification of carbon fibres. The next crucial component, for structural supercapacitors, is a structural electrolyte which should have high ionic conductivity (>1 mS/cm) and mechanical properties (Young's modulus > 1 GPa).⁶ As mentioned above, the ionic conductivity and mechanical properties, are inversely related, making this multifunctional requirement particularly challenging.⁶⁻¹⁰ This demanding relationship is especially obvious when high performance structural polymers are used, such as epoxies, where the architecture is already optimised for stiffness. Nevertheless, it has been possible⁶ to prepare electrolytes based on commercial epoxy resins (with the trade names MVR444, VTM266 and MTM57) with ionic conductivity as high as 0.8 mS/cm and Young's modulus of 0.18 GPa, by developing a bicontinuous structure where one phase is responsible for the mechanical strength and another for ionic conductivity. Varying the composition of the epoxy and electrolyte it is possible to tune morphology of the resulting structural electrolyte from traditional bicontinuous networks, in case of MVR444 and VTM266 (**Fig. 8a,b**), to more complicated structures, in case of MTM57 (**Fig. 8c,d**). The changes in morphology affect the properties of the structural electrolytes. For example, as a finer structure is formed, the ionic conductivity of the structural electrolyte decreases. The microstructure presented in **Fig. 8b** is an example of a desirable morphology, as it possesses a large scale continuous epoxy network (based on MVR444) and pores big enough for high ionic mobility. One of the benefits of using a commercial epoxy is that it allows for straightforward scale up, first to large scale composite demonstrators, and ultimately to production, as long as the addition of the electrolyte does not lead to changes in processing behaviour, for example in the curing kinetics or/and film forming ability of the epoxy resin. However, the formulation which produced the promising microstructure in **Fig. 8b** had a very short shelf life, most likely due to reactions between the imidazolium ions and the epoxy resin^{55, 56}, making it impossible to use it for structural supercapacitor manufacturing. As an alternative, formulations

based on MTM57, which resulted in more complex microstructures, were studied in the composite devices.

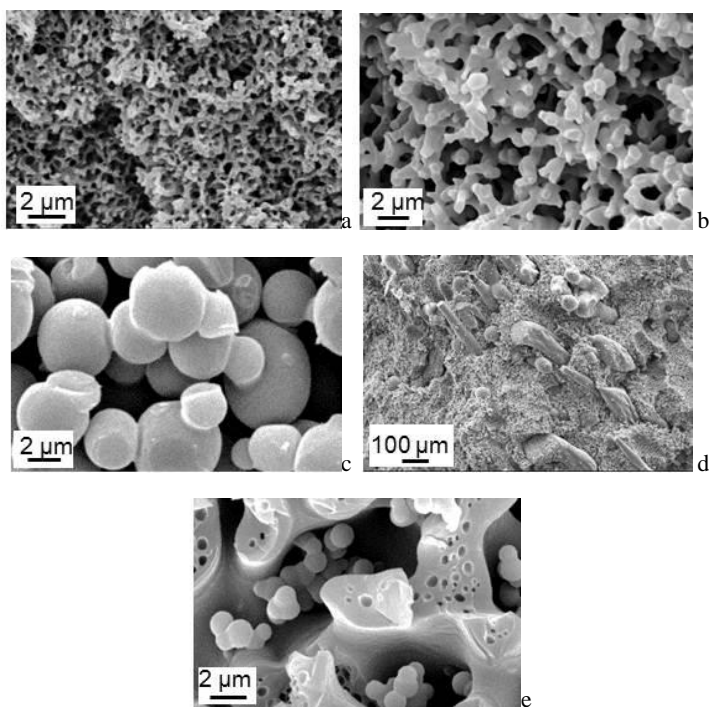


Fig. 8 Scanning electron micrographs of different types of structures; a, b—bicontinuous (a- VTM266 and b- MVR444 based); c, d, e - complex structure (MTM57 based); note that c,d is the same sample at different magnifications.

Detailed studies of the effect of electrolyte composition on the ionic conductivity and mechanical performance of the structural electrolyte based on MTM57 will be published in a separate manuscript¹⁰; however, an example of the processability issues is described here. A key issue for practical use is the need to spread the resin formulation to form a stable film that can subsequently be infused or ‘prepregged’ with the carbon fibre weave. Although formulations based on MTM57 blended with ionic liquid based electrolyte had a wider processability window (time/temperature stability) compared to MVR444 formulations, films cast from MTM57 based formulations had a tendency to reticulate[†], (**Fig. 9a**). To overcome this shortcoming, the effect of adding rheology modifiers or thixotropes was studied, using for example hydrophilic fumed silica (Cab-o-sil M5), hydrophobic fumed silica modified with polydimethylsiloxane (Aerosil R202) and “neutral” mixed mineral (Garamite 1958) additives, introduced at 1 wt.% to MTM57. Film forming properties were imaged (**Fig. 9**) on the uncured formulations that were cast and left for 1 h. The addition of a thixotrope improved film forming ability and only minimal reticulation was observed for formulations containing hydrophobic and hydrophilic thixotropes.

[†] The term “reticulation”, here, is used to describe a process of rupture or dewetting of the resin film from the substrate and can proceed to the extent of forming discrete droplets, rather than the intended continuous film.

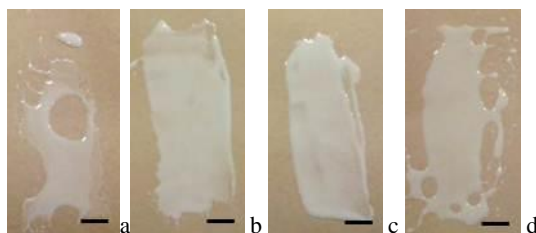
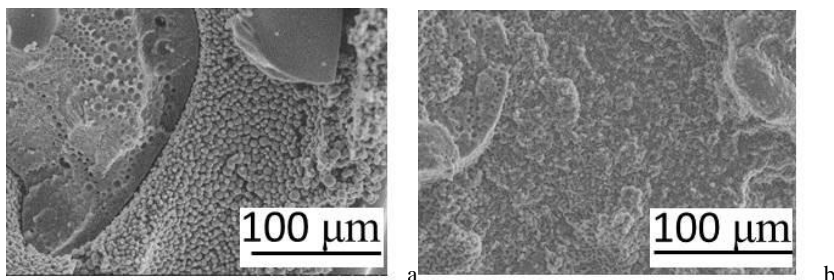


Fig. 9 Images of the films of uncured formulations based on 50/MTM57 after 1 h upon addition of thixotropes, drawn down by casting knife; a – neat; b – Aerosil; c – Cab-o-sil; d – Garamite. Scale bar is 1.3 cm.

5

However, the introduction of 1 wt.% thixotrope not only affected the film forming ability but also the morphology and properties of the resulting structural electrolytes. **Fig. 10** shows SEM images of the cured 50/MTM57 formulations containing different thixotropes. The addition of the Aerosil R202 led to formation of microstructure consisting mainly of closed pores (**Fig. 10** a,b), which resulted in a decrease in ionic conductivity values from 0.42 mS/cm for 50/MTM57 structural electrolyte to 0.004 mS/cm. The presence of Cab-o-sil and Garamite also resulted in changes in the morphology of the 50/MTM57 (**Fig. 10**c,d) but the ionic conductivity was less affected and was still 0.13 mS/cm and 0.3 mS/cm for 50/MTM57 containing Cab-o-sil and Garamite, respectively. Nanoparticulate fillers are known to modify the ionic conductivity of polymer electrolytes by providing alternative conduction paths or varying free volume. In additions, small particles are known to act as Pickering stabilisers for emulsions, with an ability to stabilise different curvature interfaces, depending on wettability.^{57, 58} The hydrophobic Aerosil is likely to promote epoxy as the continuous phase, as indeed observed. Even though the addition of the hydrophilic thixotrope had a positive effect on film forming ability, and only a small decrease in ionic conductivity of resulting structural electrolyte, the overall microstructure became less ordered. This change may be attributed to the influence of the particulate filler distribution on the phase separation during the curing process. Previous developments showed that substitution of a small amount (1 wt.%) of ionic liquid by an organic electrolyte with high dielectric constant also results in a significant change of the microstructure of the resulting structural electrolyte.¹⁰ Thus further formulation of these structural electrolyte systems is likely to be complicated, in general, by the potential to disturb the specific phase separating behaviour required. The phase behaviour in the presence of the (modified) reinforcing fibres must also be considered.



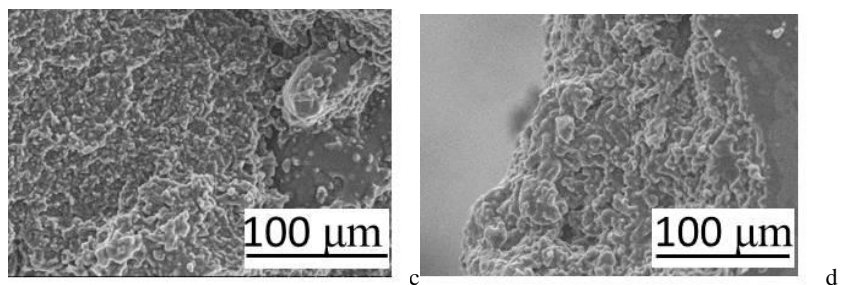


Fig. 10 Scanning electron micrographs of 50/MTM57 with and without different thixotropes; a – neat; b – Aerosil; c – Cab-o-sil; d – Garamite

5 3.6 System issues

Once the individual multifunctional components of the structural supercapacitor are developed, there are still many other issues to resolve relating to assembly, integration, manufacturing, machining/finishing, current collection, and ownership. As an example of a potential component implementation for structural supercapacitors, a variety of demonstrators have been manufactured using a pre-preg route. Due to the high viscosity of the uncured formulations of epoxy-based electrolyte, resin infusion was not applicable. Carbon fibres were separated using two glass fibre fabrics (GFs) to balance the composite in the midplane. Using the pre-preg route it was possible to manufacture not only flat laminates but also complex shapes, including components for a full size trunk lid for Volvo S80 where LEDs were powered by the structural supercapacitors, as presented in **Fig. 11**. Copper tape with conductive adhesive was chosen as a current collector and was introduced onto the carbon fibre surface prior to composite manufacturing. The copper tape does not have to be used as a long strip and it is efficient even when it is attached to the carbon fibres in a small rectangular shape with a soldered wire connection (**Fig. 11b**). The spacing and geometry of the copper contacts is fundamentally determined by the in plane conductivity of the carbon fibres electrodes and the performance of the electrochemical system (i.e. the current densities generated). Despite the effectiveness of copper contacts, there is a concern regarding the long term stability of the copper in the presence of the ionic liquid based electrolytes; different current collector materials or modification of the copper system will be needed.

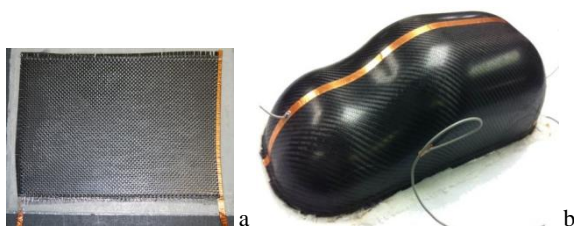




Fig. 11 Structural supercapacitor flat laminate (a); model car body (b) and trunk lid with added chrome trimming and lit LED lights (c).

Given that it will not be always possible to manufacture structural supercapacitors as a single unit, it is important to consider the connectivity and machining of the fabricated structural supercapacitors. Preliminary data showed that it is possible to drill multiple holes and trim edges without causing a short-circuit and/or compromising electrochemical performance of the structural supercapacitor. It was also possible to build stacks containing a number of single structural supercapacitor cells by separating them using layers of glass fibre/structural matrix (MTM57) pre-preg. Among many others, one question is how best to encase the manufactured structural supercapacitor without compromising its electrochemical performance, to protect the electrolyte component from the environment, specifically moisture. The most straightforward approach is use a conventional structural glass fibre pre-preg material, as long as there is no interdiffusion between the structural electrolyte and the conventional matrix of the glass fibre pre-preg.

Conclusions

Composite materials intrinsically combine the characteristics of their components; they are an ideal platform for the creation of multifunctional materials. There is an exciting opportunity to save (or redistribute) weight and volume, by combining electrical energy storage within the basic construction of a physical system. For example, in the context of hybrid/electric transport, electrical energy can be stored in the bodywork, as illustrated by the demonstrator above (Fig. 10). Similar possibilities exist in other electric vehicles (trains, trams, bikes) and in aerospace, as well as in portable electronics. In order to make these multifunctional structural power systems work effectively, multifunctional reinforcements and matrices must be developed and combined. One encouraging opportunity is the use of carbonaceous materials as both high strength/stiffness reinforcements and as electrochemical electrodes. The laminated nature of many fibre composites also facilitates many energy storing embodiments, although possibilities also exist at other length scales, such as the single fibre level⁵⁹. This discussion paper presents a strategy for preparing structural supercapacitors from a laminated architecture. For this system, the surface area of the carbonaceous layer must be maximised whilst retaining the mechanical performance of the primary carbon fibres. After comparing several methods, the use of a carbon aerogel matrix was found to be most effective, supplying the desired surface area, and maximising the utilisation of the available space. This same aerogel also offers a mechanical performance advantage by reinforcing the electrolyte matrix phase, and addressing matrix-dominated composite failures that are otherwise amplified by the compromises of the multifunctional matrix. The bicontinuous nanostructured nature of the aerogel appears to be a characteristic motif in multifunctional materials. For the

electrode, the scale of the porosity is defined by the electrochemical double layer that must be accommodated. Other requirements associated with electron/ion transport and mechanics do not appear limiting at present, although further improvements can be anticipated, particularly if hierarchical features are introduced. The multifunctional electrolyte matrix is even more demanding as it combines more inherently conflicting properties. However, the bicontinuous motif again provides encouragement. In this case, the characteristic length scale is larger, most likely defined by the diameters of the primary fibres that must be supported.

Now that the concept is demonstrated, the challenge is to increase absolute performance to practical levels; in the case of structural supercapacitors, power density remains the central target. It's worth noting, however, that the multifunctional system does not have to exceed the specific performance of both structural and electrochemical systems. It only has to offer a better performance than the combined weight of the two conventional solutions. Whilst laminated structural supercapacitors seem promising, there are many other architectures and electrochemical systems that might be considered. If suitable performance can be obtained, practical manufacturing routes will be needed for real component testing and eventual deployment. Many of the multifunctional components will bring their own challenges to formulation and processing, as highlighted above; however, these obstacles should be overcome with suitable development. Further investigation of machining, connectivity, power systems design, and through life service issues will need to be considered. Bringing such multifunctional systems to reality requires a multi-disciplinary collaboration between electrochemists, materials chemists, composite engineers and electrical power systems engineers. It is important to build mutual understanding of the requirements and challenges through dialogue and discussion.

Acknowledgement

Funding from the EU as part of the FP7 project "Storage" (Grant Agreement No. 234236) and MAST2.2 program funded by the UK Ministry of Defence are gratefully acknowledged. Authors would like to thank Mr Richard Shelton from Cytec Industrial Materials for help with sample preparation, and the wider "Storage" team for the fabrication of the Volvo boot.

References

^a *The Composites Centre, Imperial College London, London, South Kensington Campus, SW7 2AZ, U.K.; Tel: 020 7594 5825; E-mail: m.shaffer@imperial.ac.uk*

^b *NANOCYL S.A., Rue de l'Essor 4, 5060 Sambreville, Belgium*

^c *Cytec Industrial Materials, Heanor, Derbyshire, U.K.*

1. H. Pröbstle, M. Wiener and J. Fricke, *J. Porous Mater.*, 2003, 10, 213-222.
2. A. G. Pandolfo and A. F. Hollenkamp, *J. Power Sources* 2006, 157, 11-27.
3. Y. Zhang, H. Feng, X. Wu, L. Wang, A. Zhang, T. Xia, H. Dong and X. L. L. Zhang, *Int. J. Hydrogen Energy*, 2009, 34, 4889-4899.
4. G. Wang, L. Zhang and J. Zhang, *Chem. Soc. Rev.*, 2012, 41, 797-828.
5. D. D. Edie, *Carbon*, 1998, 36, 345-362.

6. N. Shirshova, A. Bismarck, S. Carreyette, Q. P. V. Fontana, E. S. Greenhalgh, P. Jacobsson, P. Johansson, M. J. Marczewski, J. Scheers, G. Kalinka, A. Kucemak, M. S. Shaffer, J. H. G. Steinke and M. Wienrich, *J. Mater. Chem. A*, 2013 doi: 10.1039/C1033TA13163G.
7. K. Matsumoto and T. Endo, *Macromolecules*, 2008, 41, 6981-6986.
- 5 8. J. F. Snyder, E. D. Wetzel and C. M. Watson, *Polymer*, 2009, 50, 4906-4916.
9. S. Wang and K. Min, *Polymer*, 2010, 51, 2621-2628.
10. N. Shirshova, A. Bismarck, E. S. Greenhalgh, P. Jacobsson, P. Johansson, M. J. Marczewski, G. Kalinka, M. S. P. Shaffer, J. H. G. Steinke and M. Wienrich, *submitted to*, 2014.
11. K. Matsumoto and T. Endo, *J. Polym. Sci. Part A: Polym. Chem.*, 2011, 49, 1874-1880.
- 10 12. K. Matsumoto and T. Endo, *Macromolecules*, 2009, 42, 4580-4584.
13. J.-P. Pascaut and R. J. J. Williams, *Epoxy Polymers*, Wiley-VCH, 2010.
14. P.-L. Kuo, W.-J. Liang and T.-Y. Chen, *Polymer*, 2003, 44, 2957-2964.
15. M. Galiński, A. Lewandowski and I. Stępnia, *Electrochim. Acta* 2006, 51, 5567-5580.
16. A. Lewandowski and A. Świdarska-Mocek, *J. Power Sources* 2009, 601-609.
- 15 17. N. D. Khupse and A. Kumar, *Indian J. Chem.*, 2010, 49A, 635-648.
18. N. Shirshova, H. Qian, M. S. P. Shaffer, J. H. G. Steinke, E. S. Greenhalgh, P. T. Curtis, A. Kucernak and A. Bismarck, *Composites: Part A*, 2013, 46, 96-107.
19. H. Qian, H. Diao, N. Shirshova, E. S. Greenhalgh, J. G. H. Steinke, M. S. P. Shaffer and A. Bismarck, *J. Colloid & Interface Sci.*, 2013, 395, 241-248.
- 20 20. H. Qian, A. Bismarck, E. S. Greenhalgh and M. S. P. Shaffer, *Composites: Part A*, 2010, 41, 1107-1114.
21. H. Qian, E. S. Greenhalgh, M. S. P. Shaffer and A. Bismarck, *J. Mater. Chem.*, 2010, 20, 4751-4762.
22. X. Zhang, D. Chang, J. Liu and Y. Luo, *J. Mater. Chem.*, 2010, 20, 5080-5085.
- 25 23. L. Jin, T. Wang, Z. Q. Feng, M. K. Leach, J. Wu, S. Mog and Q. Jiang, *J. Mater. Chem. B*, 2013, 1, 1818-1825.
24. P. West Conshohocken, 1995.
25. P. West Conshohocken, 2000.
26. H. Qian, A. R. Kucernak, E. S. Greenhalgh, A. Bismarck and M. S. P. Shaffer, *ACS Appl. Mater. Interfaces*, 2013, 5, 6113-6122.
- 30 27. J. C. Lee, B. H. Lee, B. G. Kim, M. J. Park, D. Y. Lee, I. H. Kuk, H. Chijng, H. S. Kang, H. S. Lees and D. H. Ahn, *Carbon*, 1997, 35, 1479-1484.
28. F. Severini, L. Formaro, M. Pegoraro and L. Posca, *Carbon*, 2002, 40, 735-741.
29. W. Li, S. Y. Yao, K. M. Ma and P. Chen, *Polym. Compos.*, 2013, 34, 368-375.
- 35 30. L. Liu, H. Chen and D. Pan, *Fibers & Polymers*, 2012, 13, 587-592.
31. C. Choi, J. A. Lee, A. Y. Choi, Y. T. Kim, X. Lepró, M. D. Lima, R. H. Baughman and S. J. Kim, *Adv. Mater.*, 2013, DOI: 10.1002/adma.201304736, 1-7.
32. J. A. Lee, M. K. Shin, S. H. Kim, H. U. Cho, G. M. Spinks, G. G. Wallace, M. D. Lima, X. Lepró, M. E. Kozlov, R. H. Baughman and S. J. Kim, *Nat. Commun. 4:1970*, 2013, 4.
- 40 33. C. L. Pint, N. W. Nicholas, S. Xu, Z. Sun, J. M. Tour, H. K. Schmidt, R. G. Gordon and R. H. Hauge, *Carbon*, 2011, 49, 4890-4897.
34. S. Esconjauregui, M. Fouquet, B. C. Bayer, C. Ducati, R. Smajda, S. Hofmann and J. Robertson, *ACS Nano*, 2010, 4, 7431-7436.
35. S. A. Al-Muhtaseb and J. A. Ritter, *Adv. Mater.*, 2003, 15, 101-114.
- 45 36. R. W. Pekala, *J. Mater. Sci.*, 1989, 24, 3221-3227.

-
37. J. C. Lytle, J. M. Wallace, M. B. Sassin, A. J. Barrow, J. W. Long, J. L. Dysart, C. H. Renninger, M. P. Saunders, N. L. Brandell and D. R. Rolison, *Energy Environ. Sci.*, 2011, 4, 1913–1925.
38. R. Petričević, M. Glora and J. Fricke, *Carbon*, 2001, 39, 857–867.
- 5 39. W. Li, G. Reichenauer and J. Fricke, *Carbon*, 2002, 40, 2955–2959.
40. M. Schwan and L. Ratke, *J. Mater. Chem. A*, 2013, 1, 13462–13468.
41. R. Saliger, U. Fischer, C. Herta and J. Fricke, *J. Non-Crystalline Solids*, 1998, 225, 81–85.
42. A. Szczurek, G. Amaral-Labat, V. Fierro, A. Pizzi and A. Celzard, *Sci. Technol. Adv. Mater.*, 2011, 12, 035001 (035012pp).
- 10 43. H. Tamon, H. Ishizaka, M. Mikami and M. Okazaki, *Carbon*, 1997, 35, 791–796.
44. E. A. Oyedoh, A. B. Albadarin, G. M. Walker, M. Mirzaeiian and M. N. M. Ahmad, *Chem. Eng. Transactions*, 2013, 32, 1651–1656.
45. A. M. ElKhatat and S. A. Al-Muhtaseb, *Adv. Mater.*, 2011, 23, 2887–2903.
46. D. W. Schaefer, R. Pekala and G. Beaucage, *J. Non-Crystalline Solids*, 1995, 186, 159–167.
- 15 47. S. Kondrat, C. R. Pérez, V. Presser, Y. Gogotsi and A. A. Kornyshev, *Energy Environ. Sci.*, 2012, 5, 6474–6479.
48. L. Yuan, B. Yao, B. Hu, K. Huo, W. Chen and J. Zhou, *Energy Environ. Sci.*, 2013, 6, 470–476.
49. H. An, Y. Wang, X. Wang, L. Zheng, X. Wang, L. Yi, L. Bai and X. Zhang, *J. Power Sources*, 2010, 195, 6964–6969.
- 20 50. K. S. Ryu, K. M. Kim, N. G. Park, Y. J. Park and S. H. Chang, *J. Power Sources*, 2002, 103, 305–309.
51. C. Arbizzani, M. Mastragostino and F. Soavi, *J. Power Sources*, 2001, 100, 164–170.
52. A. S. Saraç, G. Sönmez and F. Ç. Cebeci, *J. Appl. Electrochem.*, 2003, 33, 295–301.
53. G. P. Pandey and A. C. Rastogi, *Electrochim. Acta*, 2013, 87, 158–168.
- 25 54. R. Starbird, C. A. García-González, I. Smirnova, W. H. Krautschneider and W. Bauhofer, *Mater. Sci. Eng.*, 2014, 37, 177–183.
55. B. G. Soares, S. Livi, J. Duchet-Rumeau and J.-F. Gerard, *Macromol. Mater. Eng.*, 2011, 296, 826–834.
56. M. S. Heise and G. C. Martin, *Macromolecules*, 1989, 22, 99–104.
- 30 57. V. O. Ikem, A. Menner and A. Bismarck, *Langmuir*, 2010, 26, 8836–8841.
58. B. P. Binks and S. O. Lumsdon, *Phys. Chem. Chem. Phys.*, 1999, 1, 3007–3016.
59. S. Leijonmarck, T. Carlson, G. Lindbergh, L. E. Asp, H. Maples and A. Bismarck, *Compos. Sci. Technol.*, 2013, 89, 149–157.